Differentiating Arteriolosclerotic Ulcers of Martorell from Other Types of Leg Ulcers Based on Vascular Histomorphology

Julia DEINSBERGER[1,2], Jonas BRUGGER[3], Philipp TSCHANDL[2], Barbara MEIER-SCHIESSER[4], Florian ANZENGRUBER[4], Simon BOSSART[5], Stanislava TZANEVA[2], Peter PETZELBAUER[1,2], Kornelia BÖHLER[2], Helmut BELTRAMINELLI[5], Jürg HAFNER[4] and Benedikt WEBER[1,2,4,5]

[1]Skin and Endothelium Research Division (SERD), Department of Dermatology, [2]Department of Dermatology, [3]Center for Medical Statistics, Informatics and Intelligent Systems (CeMSIIS), Medical University of Vienna, Vienna, Austria, [4]Department of Dermatology, University Hospital of Zurich, Zurich, and [5]Department of Dermatology, Inselspital Bern University Hospital, University of Bern, Bern, Switzerland

Clinical differential diagnosis of arteriolosclerotic ulcers of Martorell is challenging due to the lack of clearly affirmative instrument-based diagnostic criteria. The aim of this study was to develop vascular histomorphological diagnostic criteria differentiating Martorell ulcers from other types of leg ulcers. The histomorphology of patients diagnosed with arteriolosclerotic ulcers of Martorell ($n = 67$) was compared with that of patients with venous leg ulcers, necrotizing leukocytoclastic vasculitis, pyoderma gangrenosum, and non-ulcerative controls ($n = 15$ each). In a multivariable logistic regression model, the rates of arteriolar calcification (odds ratio (OR) 42.71, 95% confidence interval (CI) 7.43–443.96, $p < 0.001$) and subendothelial hyalinosis (OR 29.28, 95% CI 4.88–278.21, $p < 0.001$) were significantly higher in arteriolosclerotic ulcers of Martorell. Arteriolar cellularity was significantly lower in Martorell ulcers than in controls (OR 0.003, 95 CI < 0.001–0.97, $p = 0.05$). However, the wall-to-lumen ratio was similar in all ulcers (OR 0.975, 95% CI 0.598–2.04, $p = 0.929$). Based on the Youden index, a wall cellularity of < 0.24 cells/100 µm² was determined as the optimum cut-off point (sensitivity 0.955, specificity 0.944). Thus, arteriolar calcification, subendothelial hyalinosis, and arteriolar cellularity revealed high discriminatory power for arteriolosclerotic ulcers of Martorell.

Key words: arteriolosclerosis; Martorell; leg ulcer; histomorphology; hyalinosis.

Accepted Apr 14, 2021; Epub ahead of print Apr 15, 2021

Acta Derm Venereol 2021; 101: adv00449.

Corr: Benedikt Weber, MD PhD, Department of Dermatology, Medical University of Vienna, Waehringer Guertel 18-20, AT-1090 Vienna, Austria. E-mail: benedikt.weber@meduniwien.ac.at

SIGNIFICANCE

The arteriolosclerotic ulcer of Martorell is characterized by necrotic leg ulcers and is associated with long-standing arterial hypertension. Differential diagnosis, however, is challenging due to a lack of clearly affirmative instrument-based diagnostic criteria. This study provides quantitative histomorphological information on arteriolar wall changes in patients with arteriolosclerotic ulcer of Martorell in comparison with ulcerative and/or non-ulcerative controls. This information may facilitate the histological diagnosis, differentiating Martorell ulcers from other types of leg ulcers, and may also contribute to a better understanding of the aetiopathogenesis of the disease.

The differential diagnosis of leg ulcers covers a wide range of diagnoses, often posing a difficult diagnostic challenge. Approximately 75% of all ulcers occur due to vascular aetiologies (1). While most leg ulcers are caused by chronic venous insufficiency (2), arterial disease represents the second leading cause (3). Besides peripheral arterial occlusive disease, stenotic diseases of the cutaneous arterioles are also significant. Originally described by Fernando Martorell in 1945 (4, 5), the arteriolosclerotic ulcer of Martorell (ASUM) is defined by several characteristics. These include location of the ulcer on the lower leg, absence of relevant macrovascular diseases, disproportionate pain, and longstanding arterial hypertension (4, 5). It is characterized by skin infarctions, presenting with deep necrotic ulcers and purple-reddish edges (6). Although the exact prevalence of ASUM remains to be elucidated, recent reports estimate that it accounts for up to 5% of all leg ulcers (7). Treatment with sharp necrosectomy, followed by vacuum-assisted negative pressure and split-thickness skin grafting, has achieved the most successful results, leading to remission in up to 90% of patients (7). However, the clinical differential diagnosis is challenging, given the lack of clearly affirmative instrument-based diagnostic criteria. Nevertheless, the differential diagnosis of ASUM harbours the risk of underdiagnosis or misdiagnosis. This is particularly disconcerting considering the reports of frequent misdiagnosis with necrotizing leukocytoclastic vasculitis or pyoderma gangrenosum (PG), potentially resulting in fatal complications due to immunosuppressive treatment (1, 7–10). Previously published diagnostic criteria (4, 5, 11), such as arterial hypertension or tissue necrosis, are not specific to ASUM. Thus, the criteria can only be used to stratify risk populations. In addition, considering that the patient population of ASUM consists primarily of multimorbid elderly patients, mixed ulcer aetiologies are frequent (7, 12–14). Uncovering a potential arteriolosclerotic component in these cases, based simply on clinical criteria, seems impossible. Therefore, histological assessment of peri-ulcerative skin biopsies

has gained increasing interest over the years. Although several authors have advocated for a bioptic assessment in suspected cases (7, 13, 15), others question its value (16, 17). Since the first report on histopathology in ASUM by Faber & Hines (18), several different "typical" histological findings in patients with ASUM have been reported. Accordingly, histological investigation of peri-ulcerative biopsy specimens evolved into an ancillary element of its diagnosis (6, 13, 19) (Table SI[1]). However, the specificity of these findings has been questioned, and remains a subject of ongoing controversial scientific discussions. Currently, there are no generally accepted and validated histological criteria for ASUM (6, 8, 16, 20, 21). In addition, no comparative study of the histomorphology of ASUM vs other types of leg ulcers has been conducted.

Therefore, this study aimed at a systematic multimodal microstructural analysis of deep skin biopsies of a large series of patients diagnosed with ASUM in 3 independent European academic dermatological wound centres. To determine the specificity of the results, the histopathological and microstructural vascular findings of patients diagnosed with ASUM were systematically compared with patients with venous leg ulcers, necrotizing leukocytoclastic vasculitis, and pyoderma gangrenosum, representing the most important clinical differential diagnoses of ASUM. In addition, findings were compared with samples from non-ulcerative skin of non-hypertensive and hypertensive controls. These results may serve as a basis for the development of histological "minimal diagnostic criteria", compatible with the diagnosis of ASUM in suspected cases.

MATERIALS AND METHODS

This study was conducted in compliance with Good Clinical Practice and the Declaration of Helsinki (22) and in accordance with the Austrian and Swiss laws. The study protocols and patient enrolment were formally approved by the local ethics committees at the Medical University of Vienna (number 2017-1171), the Canton of Zurich (number 2017-00290), and the Canton of Bern (number 2017-01216).

Case selection

This study included patients diagnosed with ASUM between 1998 and 2019 at the University Hospital of Vienna in Austria, the University Hospital of Zurich in Switzerland, and the University Hospital of Bern in Switzerland. The "ASUM" diagnosis was based on clinical and histological presentations (for details, see Appendix S1[1]). The ASUM study group was compared with the following control groups: venous leg ulcers (Venous), necrotizing leukocytoclastic vasculitis (Vasculitis), pyoderma gangrenosum (PG), non-ulcerative skin of non-hypertensive controls (Control N), and non-ulcerative skin of hypertensive controls (Control H). Skin biopsies from ulcers were performed for diagnostic reasons, according to previous recommendations on biopsies in patients with ASUM (1, 7, 13). Biopsies extended from the edge of the ulceration, including: (*i*) the healthy adjacent skin, (*ii*) the wound margin, and (*iii*) the ulcer ground itself. Biopsies were performed in an elliptical shape with a length:width ratio of > 3:1 and extended into the deep subcutaneous tissue (in most cases down to the fascia of the muscle). All non-ulcerative healthy control samples were recruited from patients receiving re-excisions after previous tumour excisions on the lower leg (without signs of the initially described neoplastic tissue).

Histological analysis

All histological specimens were initially stained with haematoxylin and eosin (H&E). Based on previous publications on the vascular histological criteria of ASUM (see Table SI[1]), the following criteria were selected for in-depth assessment of arterioles at the dermal-subcutaneous junction: (*i*) quantification of the wall-to-lumen ratio according to a method adapted from a previously published protocol (23); (*ii*) quantification of subendothelial "hyalinosis", defined as the accumulation of an amorphous, eosinophilic substance, supposedly consisting of plasma proteins, collagen, lipids and basement membrane material, in the media of arteriolar vessels, including the calculation of a cellularity index (nuclei per 100 μm^2 vessel wall surface); (*iii*) evaluation of the presence of arteriolar calcification; and (*iv*) scoring of periarteriolitis. All non-artificial intelligence histological assessments were independently performed by 2 operators (for details, see Appendix S1[1]).

Convolutional neural network analysis

To evaluate the vascular histomorphological distinguishability between ASUM and the control groups, an operator-independent analysis was performed using convolutional neural networks (CNN). The learned task of the CNN was to predict the diagnosis of a case based on a series of manually acquired histological image crops, showing vessels and their immediate surroundings at the dermal-subcutis junction. Target classes were binarized to "ASUM" and "Not ASUM". Twenty percent of the cases were split for final test evaluations. To obtain predictions for a case rather than single images, the predicted probability of "ASUM" was averaged over all images of a single case. The resulting value was measured for cases included in the validation set, and an optimal cut-off value with the highest sensitivity and specificity was set. Given that ASUM is a rare type of leg ulcer, more emphasis was placed on sensitivity; and it was provided twice the weight on this measurement. The test set included 523 images with a mean of 8 images (standard deviation ± 6.5) per lesion (for details, see Appendix S1[1]).

Discriminatory power and biostatistical analysis

For statistical comparison, Fisher's exact tests were performed for binary variables and Wilcoxon–Mann–Whitney tests for continuous variables. $p \leq 0.05$ were considered statically significant. $p \leq 0.01$ were considered highly significant. The significance levels were adjusted using a Bonferroni *post-hoc* correction (24), if applicable. Continuous variables are depicted as medians (interquartile ranges; IQR), if not indicated otherwise. A logistic regression model was defined, using the diagnosis of ASUM vs controls as the target variable and wall-to-lumen ratio, calcification, hyalinosis, and cellularity index as explanatory variables. A second model with only calcification and cellularity index as explanatory variables was defined. Receiver operating characteristic (ROC) curves were generated to test the goodness of both models. Optimal cut-off values for cellularity dependent on the presence of calcification for ASUM vs controls were obtained by calculating the Youden index in the model that included only calcification and cellularity as the explanatory variables. All statistical analyses were performed using IBM SPSS Statistics 24 (IBM Inc., Armonk, NY, USA) or R-Version 3.6.1 (25) (for details, see Appendix S1[1]).

[1]https://www.medicaljournals.se/acta/content/abstract/10.2340/00015555-3804

RESULTS

Case selection and patient characteristics

A total of 67 patients with ASUM passed the eligibility criteria. In addition, 15 patients per control group (Venous, Vasculitis, PG, Control N, Control H) were selected for the study. Altogether, 156 samples from 142 patients were analysed, resulting in an assessment of 921 arterioles.

All 67 (100%) patients with ASUM had been diagnosed with arterial hypertension, 33 (49%) had diabetes mellitus type II (DM II), 12 (18%) had renal insufficiency, 12 (18%) had peripheral arterial occlusive disease (PAOD stage I), and 16 (24%) had chronic venous disease (CVD, Clinical-Etiological-Anatomical-Pathophysiological stage <C4). All patient characteristics are summarized in Table SII[1].

Arteriolar hyalinosis

Arteriolar subendothelial hyalinosis is characterized by the deposition of glassy, amorphous fibrosclerotic material in arteriolar walls. Based on conventional H&E histology, 62 (93%) patients with ASUM showed hyalinized arteriolar vessels. This was significantly more than that in all control groups (all $p<0.001$), in which hyalinization could only be detected sporadically. The median share of hyalinized vessels in ASUM samples was 50% (28.57–70.00), which was also significantly higher than that in all other groups (0%, 0.00–0.00, $p<0.001$) (**Fig. 1**a).

Cellularity index

To quantify the fibrosclerotic subendothelial changes ("hyalinosis") resulting in acellular concentric matrix

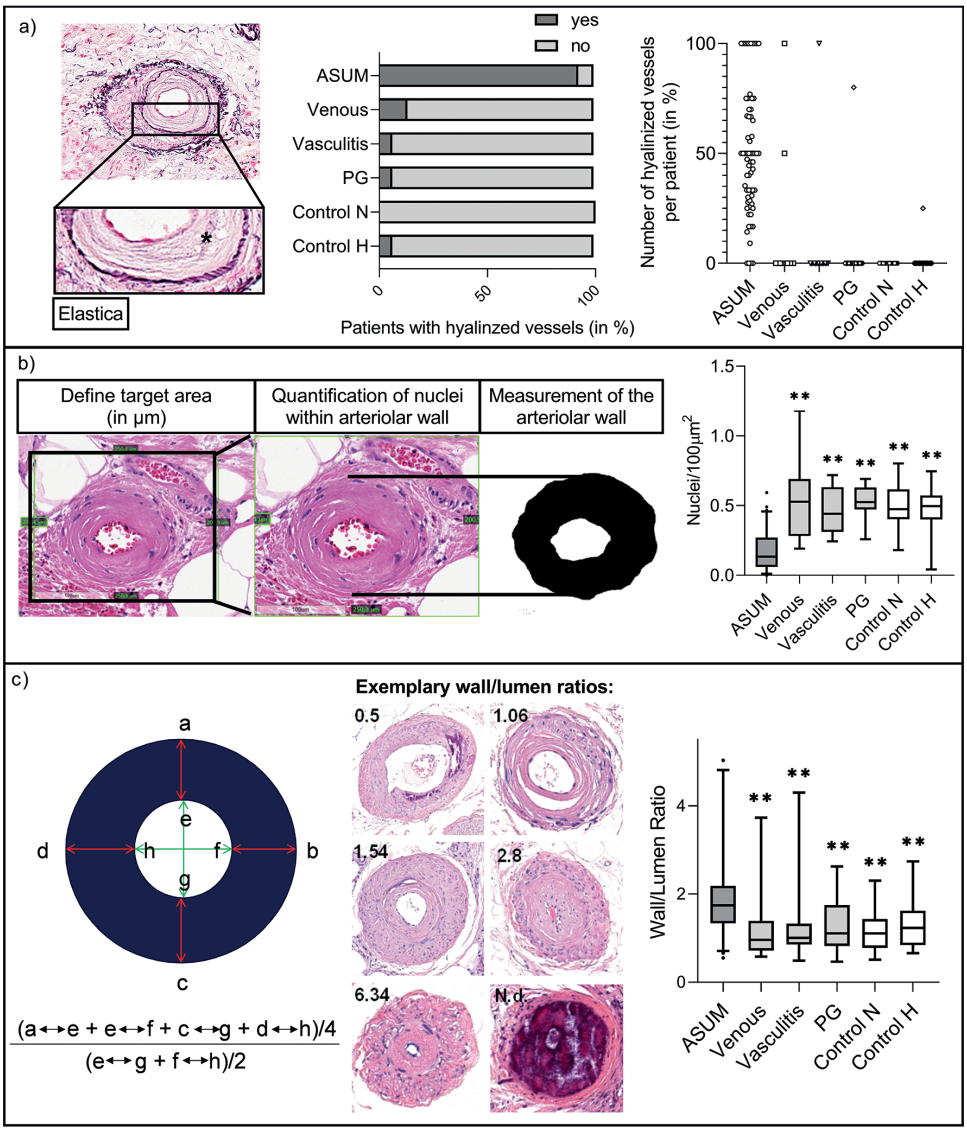

Fig. 1. Assessment of hyalinosis and arteriolar wall-to-lumen ratio. (a) Elastica staining of a dermo-hypodermal arteriole that shows subendothelial hyalinization (*asterisk* indicates hyalinized area) (*left*). Number of patients with hyalinized vessels (in %) (*middle*) and number of hyalinized vessels per patient (in %) (*right*). (b) Method for the calculation of the cellularity index (cells/100 µm^2) (*left*) and comparison of study groups (*right*), (c) Quantification of arteriolar wall/lumen ratio (AWLR) showing the formula used (*left*), examples (middle; N.d.: not definable) and AWLR of the study groups (*right*). Boxplots are plotted with median, interquartile range (IQR) and 5th–95th percentiles. Outliers are indicated as dots. ns indicates not significant, *significant ($p<0.05$) and **highly significant ($p<0.01$) results, comparing the arteriolosclerotic ulcer of Martorell (ASUM) group with the respective control group. Venous: venous leg ulcers; Vasculitis: necrotizing leukocytoclastic vasculitis; PG: pyoderma gangrenosum; Control N: non-ulcerative skin of non-hypertensive controls; Control H: non-ulcerative skin of hypertensive controls.

structures in the arteriolar wall, the cellularity index was determined. The cellularity index is defined as the number of nuclei per 100 µm² of arteriolar wall surface (Fig. 1b). The cellularity index of arterioles in patients with ASUM (0.13, 0.06–0.27) was significantly lower than that in all control groups (Venous: 0.53, 0.28–0.69, $p<0.001$; Vasculitis: 0.44, 0.31–0.63, $p<0.001$; PG: 0.52, 0.47–0.63, $p<0.001$; Control N:0.47, 0.40–0.62, $p<0.001$; Control H: 0.50, 0.40–0.57, $p<0.001$).

Wall-to-lumen ratio

To quantify and compare the luminal obstruction, the ratio between the thickness of the arteriolar wall and the lumen was determined according to a standardized protocol (23). The median arteriolar wall-to-lumen ratio (AWLR) in the ASUM samples was 1.74 (1.33–2.18). AWLRs in the control groups were 0.96 (0.72–1.39), 1.01 (0.86–1.33), 1.1 (0.82–1.75), 1.1 (0.78–1.43), and 1.23 (0.84–1.62) for Venous ulcers, Vasculitis, PG, Control N, and Control H, respectively (all $p<0.05$, Fig. 1c). However, despite the statistical significance, a more detailed analysis revealed that the quartiles of patients with ASUM and control groups showed a substantial overlap, indicating a low discriminatory power.

Calcification

Arteriolar calcification was present in 51 (76%) patients with ASUM. In all control groups, arteriolar calcification could only be seen sporadically compared with that in the ASUM group (all $p<0.001$, **Fig. 2**a).

Periarteriolitis

Periarteriolitis is characterized by immune cell infiltrates next to the arteriolar wall. In 61 (91%) patients with ASUM, periarteriolitis was detected in at least one vessel, as well as in 10 (67%), 13 (87%), 15 (100%), 7 (47%) and 6 (40%) patients of the Venous, Vasculitis, PG, Control N, and Control H groups, respectively. The mean percentage of affected vessels was 73% (±31.3), 44% (±41.3), 82% (±35.9), 98.7% (±5.2), 22.1% (±28.3) and 18.9% (±31.4) in the ASUM, Venous, Vasculitis, PG, Control N, and Control H groups, respectively (Fig. 2c). To quantify the severity, periarteriolitis was graded from 0 (no periarteriolitis) to 4 (severe periarteriolitis). The median severity scores were 1.45 (0.79–1.85), 0.56 (0.00–2.67), 1.00 (1.00–2.00), 3.00 (2.20–4.00), 0.00 (0.00–0.50) and 0.00 (0.00–0.25) for the ASUM, Venous, Vasculitis, PG, Control N, and Control H groups, respectively. In both assessments,

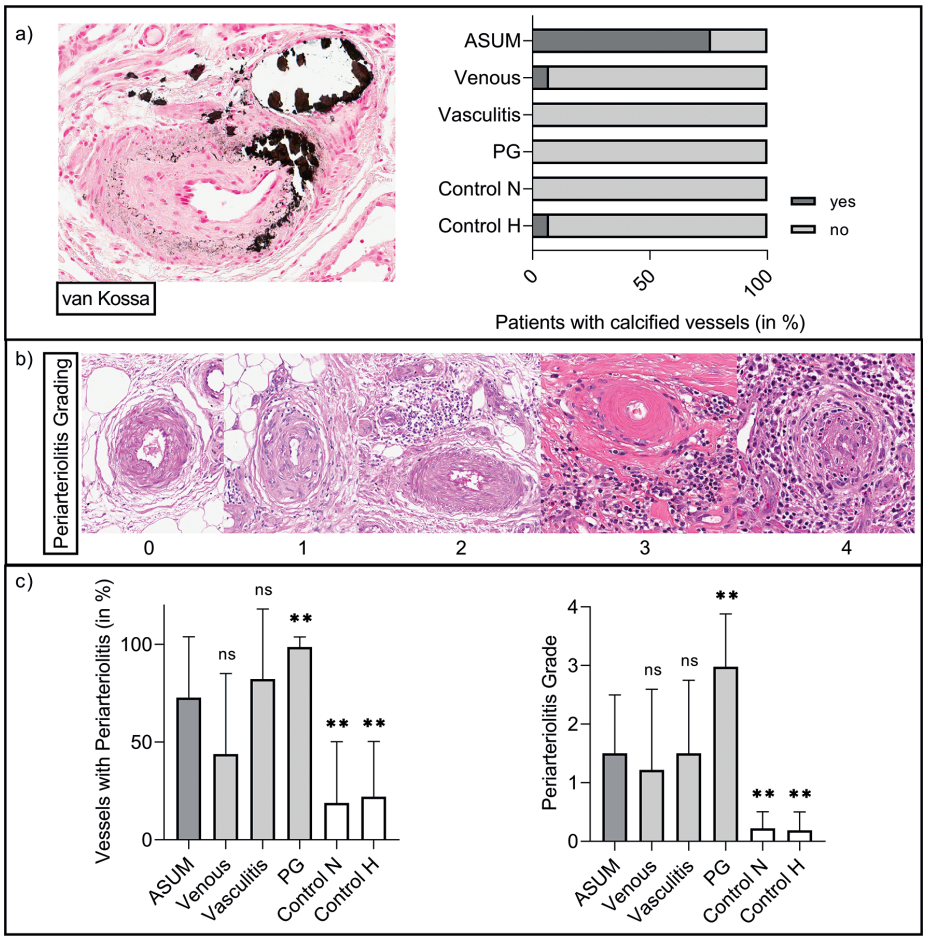

Fig. 2. Assessment of calcification and periarteriolitis. (a) von Kossa-stained arteriolosclerotic ulcer of Martorell (ASUM) sample showing an arteriolar vessel with calcification (*left*) and number of patients with calcified vessels (in %) (*right*), (b) Periarteriolitis grading scale from 0 (no periarteriolitis) to 4 (severe periarteriolitis) (c) Number of vessels with periarteriolitis per patient (in %, *left*) and mean periarteriolitis grade of vessels per patient (*right*). Column bar graphs are displayed with mean and standard deviation. ns: not significant, *significant ($p<0.05$) and **highly significant ($p<0.01$) results comparing the ASUM group with the respective control group. Magnification: a) von Kossa staining: 400x. b) Periarteriolitis Grading: 0, 1, 2: 250x; 3, 4: 400x. Venous: venous leg ulcers; Vasculitis: necrotizing leukocytoclastic vasculitis; PG: pyoderma gangrenosum; Control N: non-ulcerative skin of non-hypertensive controls; Control H: non-ulcerative skin of hypertensive controls.

only the differences in the ASUM group compared with those in the PG, Control N, and Control H groups were statistically significant ($p<0.001$, Fig. 2c).

Convolutional neural network analysis

Convolutional neural network (CNN) analysis was performed to evaluate the histomorphological distinguishability between the ASUM and control groups. Automated predictions of 523 test images showed a mean sensitivity of 0.882 (95% CI 0.834–0.931), specificity of 0.7 (95% CI 0.446–0.954), and an area under the ROC curve (AUC) of 0.889 (95% CI 0.824–0.995). **Fig. 3**a shows the application of Grad-CAM (26) to image crops, where image regions with the 200 highest and lowest activation values for ASUM were extracted to interpret probably useful distinctive features, as perceived by the CNN. Manual qualitative *post-hoc* analysis of the resulting image regions with the highest activation for ASUM showed hypocellular (81%), lamellar convex (19%), and strongly eosinophilic (3.5%) features, corresponding to hyalinosis and basophilic regions indicating calcification (13.5%).

Discriminatory power and biostatistical analysis

A logistic regression model was defined using the diagnosis of ASUM vs controls as target variable and wall-to-lumen ratio, calcification, hyalinosis and cellularity index as explanatory variables. A second model with only calcification and cellularity index as explanatory variables was calculated. Odds ratios (OR) for calcification, hyalinosis, and cellularity were significantly different from 1. Calcified vessels were more likely found in patients with ASUM (OR 42.7, 95% CI 7.4–444.0, $p<0.001$). Similarly, patients with ASUM were more likely to have vessels with hyalinosis (OR 29.3, 95% CI 4.9–278.2, $p<0.001$). Patients with ASUM showed lower cellularity (OR 0.003, 95% CI <0.001–0.97, $p=0.05$). The AWLR did not significantly differ (OR 0.98, 95% CI 0.60–2.04, $p=0.929$). The AUC values of 0.983 (all parameters included) and 0.971 (only cellularity and calcification) suggest a good diagnostic ability of both models (Fig. 3b).

The optimal cut-off values for cellularity based on the Youden index were 0.24 (if no calcification was observed) and 0.64 (if calcification was observed). Classifying individuals with lower cellularity than the

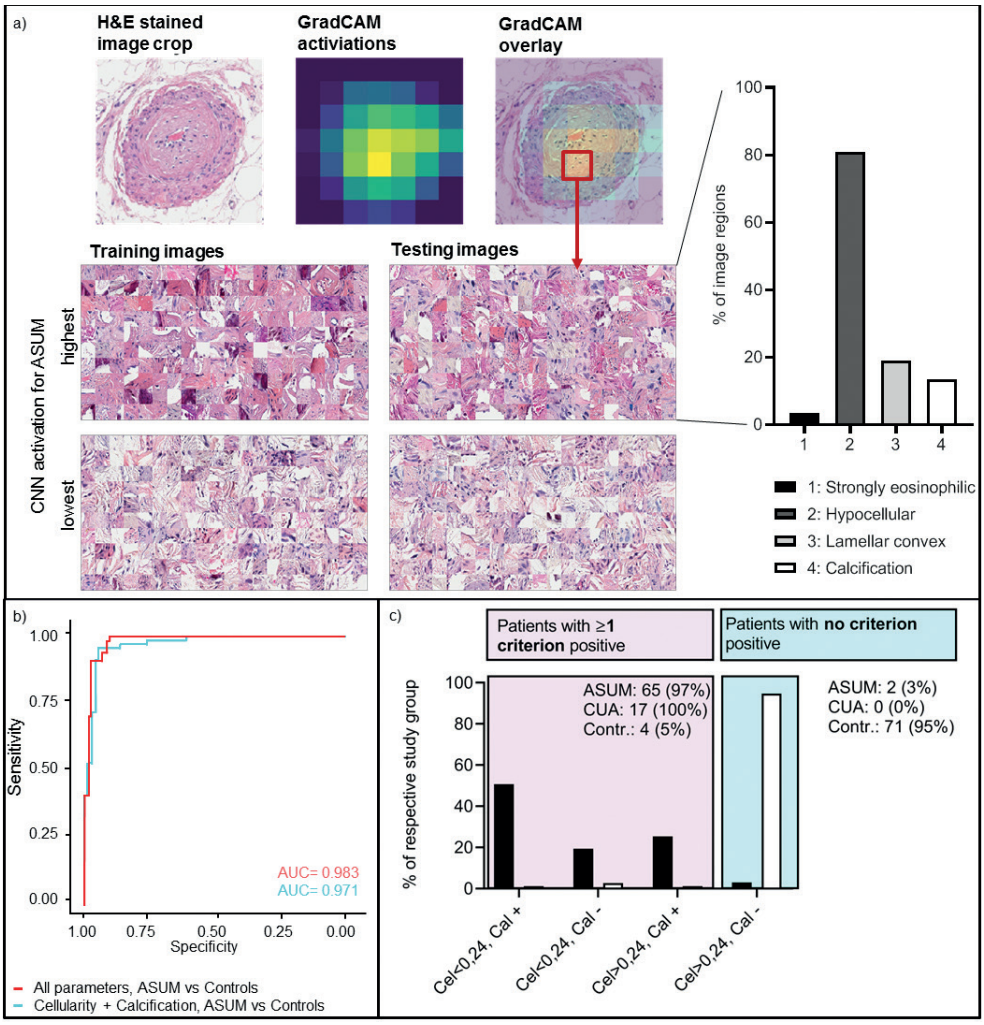

Fig. 3. Convolutional neural network (CNN) analysis and logistic regression model. (a) Analysis of a convolutional neural network trained to distinguish arteriolosclerotic ulcer of Martorell (ASUM) from controls, based on vessel-centred image crops. Grad-CAM (26) analysis for ASUM-prediction on an example image (*upper left*) shows the highest activation within the vessel wall (*upper middle* and *right*). Extraction of the 200 image areas of the highest and lowest ASUM-activation of all training and test images (*lower left* and *middle*) indicate more eosinophilic colour and hypocellularity as objective distinctive features. Manual review of highly ASUM-activated areas of the test images is shown on the *right*, (b) Receiver operating characteristic (ROC) curve of the logistic regression model with the diagnosis ASUM vs controls as the target variable and wall/lumen ratio, calcification, hyalinosis and cellularity as the explanatory variables (*red*) and with cellularity and calcification as explanatory variables (*blue*). (c) Evaluation of ASUM and controls using 2 criteria, cellularity index (Cel) <0.24 and presence of calcification (Cal). *Purple box* indicates patients, who fulfil at least 1 criterion. The *blue box* indicates patients, who fulfil none of the criteria. AUC: Area under the curve.

above-mentioned thresholds will result in a sensitivity of 0.955 and a specificity of 0.944 for the diagnosis of ASUM. When "cellularity < 0.24" and "presence of calcification" were applied as criteria, 97% of patients with ASUM and only 5.3% of the controls fulfilled at least one of the criteria (Fig. 3c and Fig. S1[1]).

The presence of hyalinosis and calcification in patients with ASUM did not differ significantly depending on the comorbidities, including DM II, chronic kidney disease, PAOD, and CVI. However, calcification of arterioles was significantly more frequent in patients taking vitamin K antagonists (92% vs 67%; $p = 0.036$; **Fig. 4**).

DISCUSSION

ASUM represents an important differential diagnosis of leg ulcers of vascular origin. However, its diagnosis is challenging, given the lack of clearly affirmative instru-

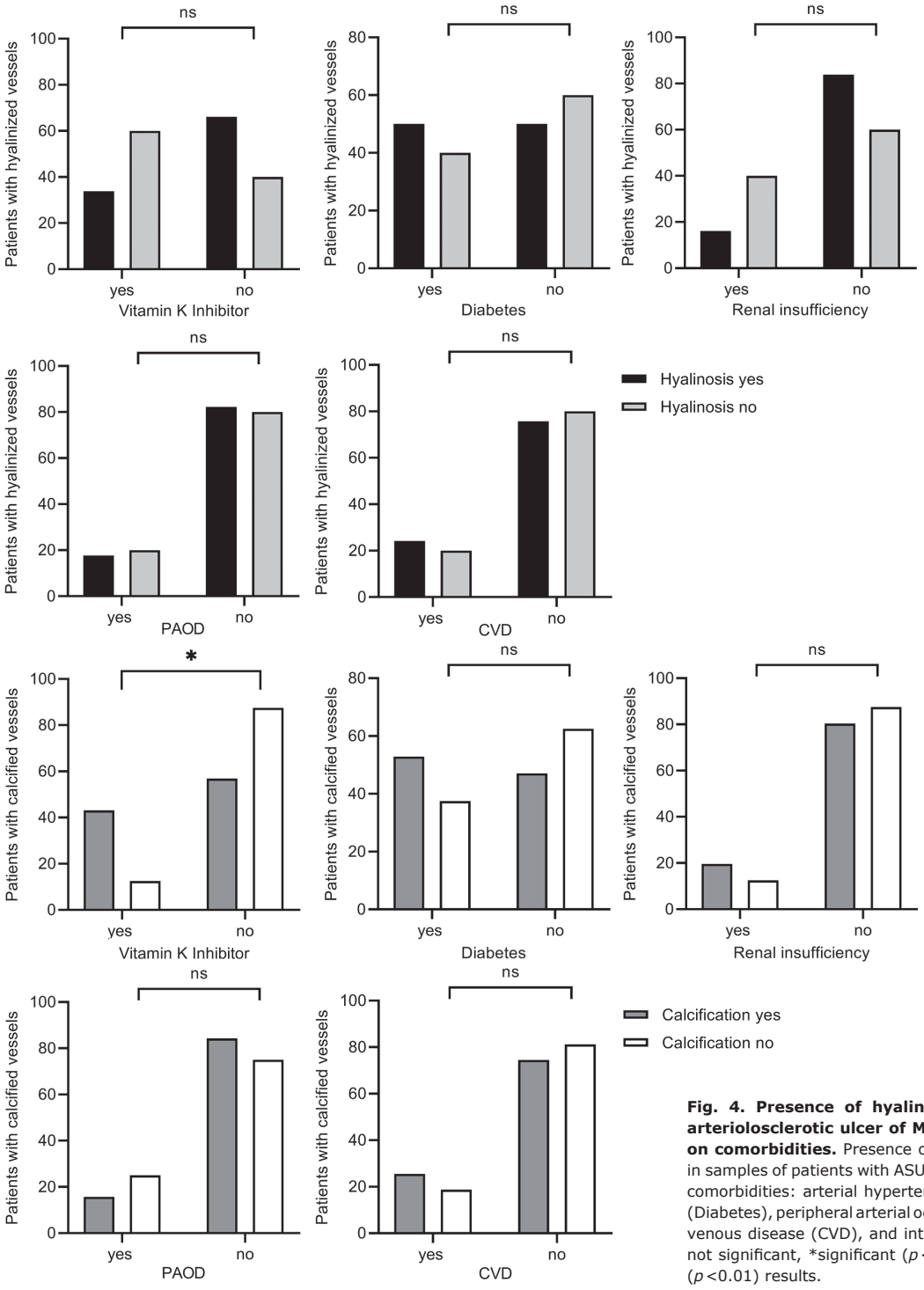

Fig. 4. Presence of hyalinization and calcification in arteriolosclerotic ulcer of Martorell (ASUM), dependent on comorbidities. Presence of hyalinization and calcification in samples of patients with ASUM is dependent on the following comorbidities: arterial hypertension, diabetes mellitus type II (Diabetes), peripheral arterial occlusive disease (PAOD), chronic venous disease (CVD), and intake of vitamin K inhibitors. ns: not significant, *significant ($p < 0.05$) and **highly significant ($p < 0.01$) results.

ment-based diagnostic criteria. Consequently, ASUM poses a major risk of underdiagnosis or misdiagnosis, which is particularly disconcerting considering reports of misdiagnosis with other types of leg ulcers, potentially resulting in fatal complications due to immunosuppressive treatment (1, 7–10). Although several different histological findings in patients with ASUM have been reported, there are no generally accepted, validated histological criteria for ASUM available to date (6, 8, 16, 20, 21). The presence of "stenosing arteriolosclerosis", composed of hyalinosis, muscular hypertrophy, and calcification, has been considered the histological hallmark of ASUM by several authors (6, 13, 18, 19). Hyalinosis, which is characterized by the accumulation of an amorphous eosinophilic substance, supposedly consisting of plasma proteins, collagen, lipids, and basement membrane material, in the media of arteriolar vessels, is mostly accompanied by the loss of smooth muscle cells involving hardening and loss of elasticity of the arteriolar wall (27–29). Although it has been reported by several authors (7, 13, 20, 30, 31), the term "hyalinosis" represents a rather unspecific term. The exact molecular composition of these hyaline subendothelial deposits in ASUM has not been elucidated thus far. However, given the reports on similar histological changes in some non-ulcerative hypertensive patients (23), the specificity of these findings has been questioned (8, 16).

The aim of the present study was to perform a systematic multimodal microstructural comparative analysis of skin biopsies of a large series of patients diagnosed with ASUM and different ulcerative and non-ulcerative control groups. To achieve a maximum number of typical ASUM cases, the patient material from 3 independent European wound care centres was combined. Stringent eligibility criteria were initially applied to exclude ulcers that may also harbour another, particularly macrovascular, aetiological component. To investigate their specificity, the histological signs of arteriolosclerosis and -stenosis found in ASUM were compared with the most important clinical differential diagnoses of ASUM, namely venous leg ulcers, necrotizing leukocytoclastic vasculitis, pyoderma gangraenosum, and non-ulcerative non-hypertensive as well as hypertensive controls. A multivariable regression model with ASUM as the target variable and wall-to-lumen ratio, calcification, hyalinosis, and cellularity as explanatory variables showed that calcified vessels occurred significantly more often in patients with ASUM in addition to vessels with hyalinosis. While the AWLR did not significantly differ, the cellularity indices were significantly higher in all control groups. Therefore, arteriolar calcification, subendothelial hyalinosis, and decreased cellularity (with a cellularity index of <0.24 cells/100 μm^2 representing the optimum cut-off value based on the Youden index) revealed high discriminatory power for ASUM compared with that for ulcerative and non-ulcerative controls.

These observations were supported by an operator-independent CNN analysis, as the image regions with highest activation for ASUM showed hypocellular, lamellar convex, and eosinophilic regions corresponding to hyalinosis, and strongly basophilic regions corresponding to calcification.

The presence of hyalinosis and calcification did not differ based on comorbidities, including DM II, chronic kidney disease, PAOD, and CVI. However, calcification of arterioles was significantly more frequent in patients taking vitamin K antagonists. This is consistent with the hypothesis that vitamin K deficiency promotes vascular calcification by decreasing the activation of matrix Gla-protein, which is synthesized by vascular smooth muscle and endothelial cells and acts as a strong inhibitor of vascular calcification by keeping the extracellular matrix free of calcium deposits (32–34).

Study limitations

This study has several limitations. One major limitation is the retrospective study design. The patient data was collected from 3 different study centres and finally combined to achieve the maximum number of cases. In addition, differences in diagnostic work-up and histological sample processing cannot be fully excluded. Due to the rather limited incidence of the disease, patients with ASUM were collected over a long study period of 21 years, which brings about a heterogeneous study population, particularly regarding therapeutic measures of ASUM as well as of secondary factors, such as the use of anticoagulants or the use of different standard antihypertensive drugs, which has changed over the years. These differences in pharmaceutical interventions might have also had an impact on the disease course and histological findings, such as the presence of arteriolar calcification. Several patients had to be excluded *a priori*, due to the presence of a relevant concomitant macrovascular disease. However, this selection process also represents a potential bias with regard to the extrapolation of the findings to a non-selected patient population in daily clinical routine.

Conclusion

This study provides quantitative histomorphological information on arteriolar wall changes in patients with ASUM in comparison with that in ulcerative and/or non-ulcerative controls. Overall, both manual and operator-independent computational histomorphological analysis suggest arteriolar calcification and hyalinosis (quantified by decreased wall cellularity, particularly <0.24 cells/100 μm^2) as the main discriminatory parameters in the microstructural differential diagnosis of ASUM from other leg ulcer entities. This may facilitate the histological diagnosis in unclear cases in the future. However, this may also contribute to a better understanding of

the aetiopathogenesis of the disease, involving a loss of cellularity in the subendothelial arteriolar wall. Future studies will have to further unravel the exact molecular composition of this acellular fibrosclerosis. This would allow for: (*i*) a more detailed understanding of the underlying pathophysiological mechanisms, (*ii*) a potential molecular differentiation from the vascular acellular fibrosclerosis observed in other types of diseases, such as diabetic ulcers (10), and (*iii*) the development of future therapeutic strategies targeting these vascular deposits in affected patients.

ACKNOWLEDGEMENTS

The authors thank Mark S. Wienand from the Department of Dermatology at Inselspital Bern, Klaudia Schossleitner, Silvio Holzner, and Sophie Bromberger from the Department of Dermatology at the Medical University of Vienna for their scientific advice and input. We thank the NVIDIA Corporation for donation of the Titan Xp GPU used for CNN analyses in this research. We thank the team of the Center for Medical Statistics, Informatics and Intelligent Systems (CeMSIIS), Medical University of Vienna, Vienna, Austria for their assistance and help with the biostatistical data analysis.

Funding. The authors thank the following funding institutions for their support: Austrian Science Fund (FWF; P-30615), Medical Scientific Fund of the Mayor of the City of Vienna (MA-GMWF-501912-2019), Vienna Science and Technology Fund (WWTF; LS18-080), and institutional funding of the Medical University of Vienna, Austria.

The authors have no conflicts of interest to declare.

REFERENCES

1. Alavi A, Mayer D, Hafner J, Sibbald RG. Martorell hypertensive ischemic leg ulcer: an underdiagnosed Entity(c). Adv Skin Wound Care 2012; 25: 563–572; quiz 573–564.
2. Mekkes JR, Loots MA, Van Der Wal AC, Bos JD. Causes, investigation and treatment of leg ulceration. Br J Dermatol 2003; 148: 388–401.
3. Martinengo L, Olsson M, Bajpai R, Soljak M, Upton Z, Schmidtchen A, et al. Prevalence of chronic wounds in the general population: systematic review and meta-analysis of observational studies. Ann Epidemiol 2019; 29: 8–15.
4. Martorell F. Ulcus cruris hypertonicum. Med Klin 1957; 52: 1945–1946.
5. Martorell F. Hypertensive ulcer of the leg. J Cardiovasc Surg (Torino) 1978; 19: 599–600.
6. Vuerstaek JD, Reeder SW, Henquet CJ, Neumann HA. Arteriolosclerotic ulcer of Martorell. J Eur Acad Dermatol Venereol 2010; 24: 867–874.
7. Hafner J, Nobbe S, Partsch H, Lauchli S, Mayer D, Amann-Vesti B, et al. Martorell hypertensive ischemic leg ulcer: a model of ischemic subcutaneous arteriolosclerosis. Arch Dermatol 2010; 146: 961–968.
8. Salcido RS. Enduring eponyms: the mystery of the Martorell ulcer. Adv Skin Wound Care 2012; 25: 535.
9. Rouphael NG, Ayoub NM, Tomb RR. Skin ulcers misdiagnosed as pyoderma gangrenosum. N Engl J Med 2003; 348: 1064–1066; author reply 1064–1066.
10. Malhi HK, Didan A, Ponosh S, Kumarasinghe SP. Painful leg ulceration in a poorly controlled hypertensive patient: a case report of martorell ulcer. Case Rep Dermatol 2017; 9: 95–102.
11. Graves JW, Morris JC, Sheps SG. Martorell's hypertensive leg ulcer: case report and concise review of the literature. J Hum Hypertens 2001; 15: 279–283.
12. Kolios AGA, Hafner J, Luder C, Guenova E, Kerl K, Kempf W, et al. Comparison of pyoderma gangrenosum and Martorell hypertensive ischaemic leg ulcer in a Swiss cohort. Br J Dermatol 2018; 178: e125–e126.
13. Hafner J. Calciphylaxis and Martorell hypertensive ischemic leg ulcer: same pattern – one pathophysiology. Dermatology 2016; 232: 523–533.
14. Henderson CA, Highet AS, Lane SA, Hall R. Arterial hypertension causing leg ulcers. Clin Exp Dermatol 1995; 20: 107–114.
15. Serpa MJ, Franco S, Repolho D, Araujo I, Mateus S, Baptista AM, et al. A challenging diagnosis of leg ulcer. Eur J Case Rep Intern Med 2018; 5: 000952.
16. Leu HJ. Hypertensive ischemic leg ulcer (Martorell's ulcer): a specific disease entity? Int Angiol 1992; 11: 132–136.
17. Lima Pinto AP, Silva NA, Jr, Osorio CT, Rivera LM, Carneiro S, Ramos ESM, et al. Martorell's ulcer: diagnostic and therapeutic challenge. Case Rep Dermatol 2015; 7: 199–206.
18. Hines EA, Jr., Farber EM. Ulcer of the leg due to arteriolosclerosis and ischemia, occurring in the presence of hypertensive disease (hypertensive-ischemic ulcers). Proc Staff Meet Mayo Clin 1946; 21: 337–346.
19. Schnier BR, Sheps SG, Juergens JL. Hypertensive ischemic ulcer. A review of 40 cases. Am J Cardiol 1966; 17: 560–565.
20. Shutler SD, Baragwanath P, Harding KG. Martorell's ulcer. Postgrad Med J 1995; 71: 717–719.
21. Monfort JB, Cury K, Moguelet P, Chasset F, Bachmeyer C, Frances C, et al. Cutaneous arteriolosclerosis is not specific to ischemic hypertensive leg ulcers. Dermatology 2018; 234: 194–197.
22. World Medical Association Declaration of Helsinki: ethical principles for medical research involving human subjects. JAMA 2013; 310: 2191–2194.
23. Farber EM, Hines EA. The arterioles of the skin in essential hypertension. J Invest Dermatol 1947; 9: 285–298.
24. Armstrong RA. When to use the Bonferroni correction. Ophthalmic Physiol Opt 2014; 34: 502–508.
25. Team RC. A Language and environment for statistical computing. Vienna, Austria: R Foundation for Statistical Computing, 2019. [Accessed December 18, 2019] Available from: https://www.R-project.org/.
26. Selvaraju RR, Cogswell M, Das A, Vedantam R, Parikh D, Batra D. Grad-CAM: Visual Explanations from Deep Networks via Gradient-Based Localization. Avaliable from: https://ieeexplore.ieee.org/document/8237336. 2017 IEEE International Conference on Computer Vision (ICCV). Venice, 2017: p. 618–626.
27. Gamble CN. The pathogenesis of hyaline arteriolosclerosis. Am J Pathol 1986; 122: 410–420.
28. Mencke R, Umbach AT, Wiggenhauser LM, Voelkl J, Olauson H, Harms G, et al. Klotho deficiency induces arteriolar hyalinosis in a trade-off with vascular calcification. Am J Pathol 2019; 189: 2503–2515.
29. Dagregorio G, Guillet G. A retrospective review of 20 hypertensive leg ulcers treated with mesh skin grafts. J Eur Acad Dermatol Venereol 2006; 20: 166–169.
30. De Andres J, Villanueva VL, Mazzinari G, Fabregat G, Asensio JM, Monsalve V. Use of a spinal cord stimulator for treatment of Martorell hypertensive ulcer. Reg Anesth Pain Med 2011; 36: 83–86.
31. Conde Montero E, Guisado Munoz S, Perez Jeronimo L, Peral Vazquez A, Montoro Lopez JJ, Hocajada Reales C, et al. Martorell hypertensive ischemic ulcer successfully treated with punch skin grafting. Wounds 2018; 30: E9–E12.
32. Nigwekar SU, Bloch DB, Nazarian RM, Vermeer C, Booth SL, Xu D, et al. Vitamin K-dependent carboxylation of matrix gla protein influences the risk of calciphylaxis. J Am Soc Nephrol 2017; 28: 1717–1722.
33. Luo G, Ducy P, McKee MD, Pinero GJ, Loyer E, Behringer RR, et al. Spontaneous calcification of arteries and cartilage in mice lacking matrix GLA protein. Nature 1997; 386: 78–81.
34. Schurgers LJ, Uitto J, Reutelingsperger CP. Vitamin K-dependent carboxylation of matrix Gla-protein: a crucial switch to control ectopic mineralization. Trends Mol Med 2013; 19: 217–226.